Relationship between brightness and roughness of polypropylene abraded surfaces

Adrien van Gorp, Maxence Bigerelle, Denis Najjar

Relationship Between Brightness and Roughness of Polypropylene Abraded Surfaces

Adrien Van Gorp,[1] Maxence Bigerelle,[2] Denis Najjar[3]
[1] *Arts & Metiers ParisTech; Mechanics, Surfaces and Materials Processing (MSMP), 8, Boulevard Louis XIV, Lille 59046, France*
[2] *Laboratory of Industrial and Human Automation Control, Mechanical Engineering and Computer Science, UMR CNRS 8201, Université De Valenciennes, Valenciennes 59313, France*
[3] *EC Lille, LML, CNRS FRE 3723, Université De Lille Nord De France, Villeneuve D'ascq 59650, France*

This article proposes to analyze the relation between gloss and roughness of surfaces of polypropylene samples abraded at different magnitudes. Experiments consist of mechanical polishing at different grades, roughness profiles measurement, and specular light reflectometry with three incidence angles of resulting surfaces. About 100 roughness parameters were considered in this investigation and an original statistical methodology combining the conventional one-way ANOVA to the recent and powerful Computer Based Bootstrap Method (CBBM) is presented to select which of them is the most relevant, first, to characterize the polypropylene surfaces abraded at different magnitude and, second, to model the physical interaction of these abraded surfaces with a white light beam. The statistical treatment of the experimental results of this investigation shows that the fractal dimension is the most relevant roughness parameter in the two cases. As far as the optical properties are concerned, it is shown that the fractal dimension of an abraded surface is closely related to the local curvature radii of peaks which are known to play a major role in physical interactions with a white light beam.

INTRODUCTION

Plastics industry is more and more constrained to produce parts with good visual aspect. In this way, the question of the surface resistance to scratch during the part life time is of prime importance. Some authors have analyzed this point to highlight a relation between surface roughness evolution induced by scratching and its consequence on the visual aspect perception. In dentistry science, some authors studied this relation by assessing tribological behavior of dental restorative resins but without modeling it [1, 2]. Others made statistics to compare the visual perception of surface roughness [3, 4]. The main conclusion of this later work is the subjective aspect of visual perception which can include variability in studies. Last, some authors try to model the relation by using a linear model [5], an exponential relation [6], or a power law [7]. These models are designed by using gloss measurements and more current roughness parameters like the arithmetic average roughness (R_a), the root-mean square roughness (R_q), or the fractal complexity proposed by V. Briones et al. [6].

Correspondence to: M. Bigerelle; e-mail: maxence.bigerelle@univ-valenciennes.fr

In routine production environment, whatever its expected functional properties, it is common to quantify the surface morphology using the arithmetic average roughness R_a, the root-mean square roughness R_q but also the peak-to-valley roughness R_t or the number of peaks N_p. If such conventional roughness parameters are usually considered to qualify the surface morphology of manufactured products, it must be pointed out that the morphology of a surface can be characterized by many other roughness parameters. Deciding without preconceived opinion which of these various parameters is the most relevant for describing the correlation between a surface morphology and a particular functional property is a difficult task of paramount importance. The relevance of each parameter is usually assessed from the conclusions of statistical tests based on inference assumptions. Because of the inflation of the roughness parameter number termed by Whitehouse, the "parameter rash" [8], the proportional number of traditional statistical tests that have to be performed becomes tedious and the risk of violating the inferred assumptions (i.e., the risk of asserting wrong conclusions) increases. This "parameter rash" was at the origin of the creation and development in our team of a specific computer routine called MESRUG that can first calculate a hundred roughness parameters and, second, can statistically estimate their relative relevance faced to a correlation with a particular functional property [9–11]. In this computer routine, the recent and powerful Computer Based Bootstrap Method (CBBM) is combined to usual statistical analyses to assess quantitatively and automatically the relative relevance of a hundred roughness parameters with regard to a given correlation with a functional property.

The aim of this article is to compare about 100 roughness parameters to make the link with gloss measurements and select the most relevant one by using original statistical techniques. The results are discussed with regards to the selected model (linear or exponential) before trying to give a physical interpretation. The experimental support is made of polypropylene surfaces abraded with different grades to produce different roughness.

EXPERIMENTS AND METHODS

Preparation of Polypropylene Abraded Surfaces and Measurements

The polypropylene abraded surfaces were prepared using an automatic grinding machine. Seven samples of 50 × 50 mm^2 size were ground with various abrasive SiC paper grades 80, 180, 220, 320, 500, 800, and 1,200 to create various degrees of abraded surfaces; each number corresponding to the number of grain per cm^2. This grinding procedure leads to typical surface

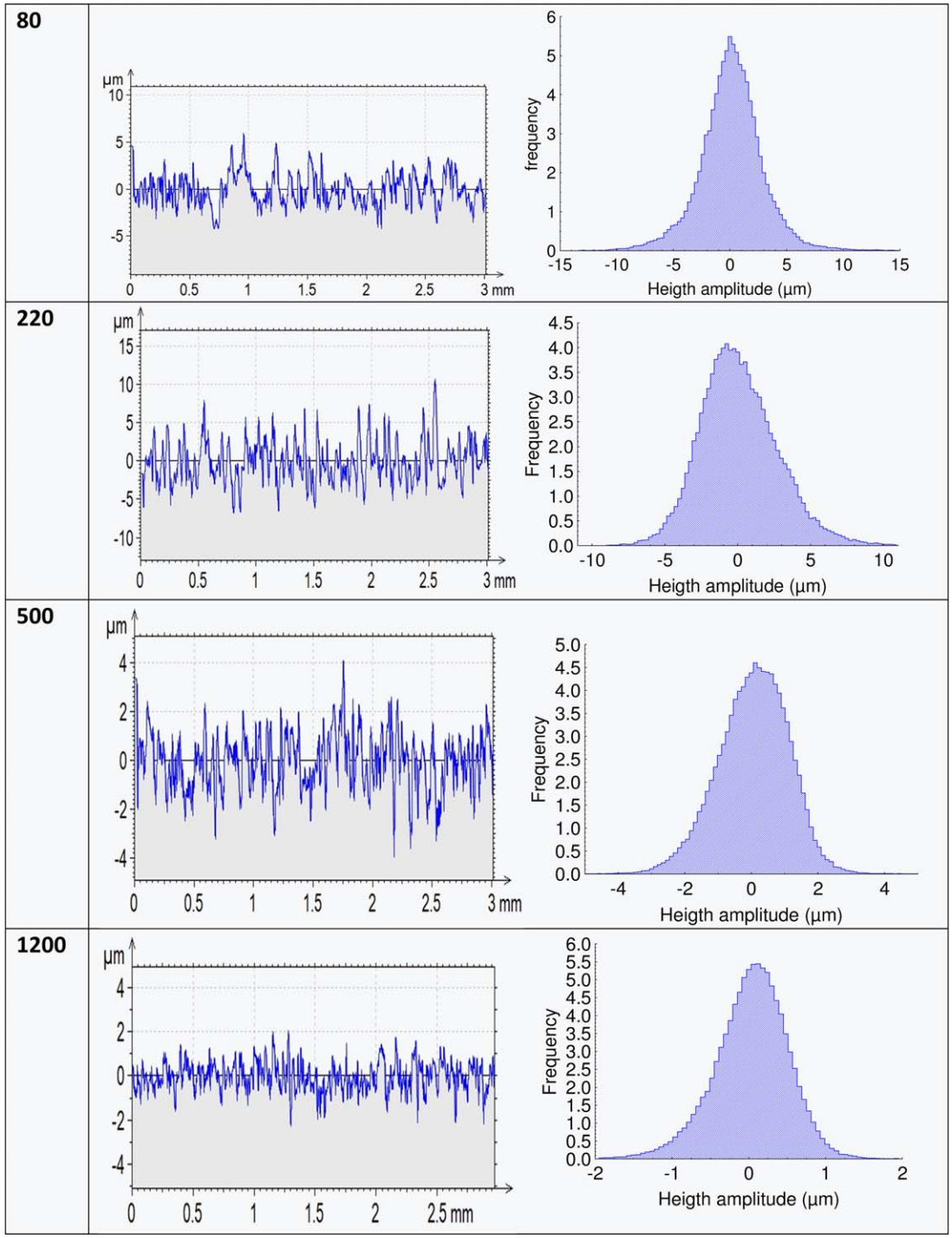

FIG. 1. On the left, roughness profiles for polypropylene surfaces abraded with grit size paper 80, 220, 500, and 1,200. On the right, height amplitude histograms computed from all roughness profiles (50 samples). [Color figure can be viewed in the online issue, which is available at wileyonlinelibrary.com.]

morphologies with an isotropic texture consisting of randomly distributed scratches by looking it to naked eye.

Surface topography of the samples has been characterized by means of a three-dimensional (3D) tactile roughness profilometer KLA TENCOR P10. This latter device consists of a diamond tip with a 2 μm rounded-end having a 10 nm vertical resolution according to the manufacturer. For each sample and paper grade, fifty profiles have been randomly recorded onto the surface using a load of 5 mg. Each recorded profile consists of 15,000 points equally spaced by a 0.2 μm distance.

Figure 1 shows the typical 2D profiles and the associated histogram of the heights of profiles for grades 80, 220, 500, and 1,200. The magnification of the vertical scale relative to the horizontal one should be noted for each profile as well as the bell shape of the histograms characteristic of the Gaussian distribution.

The specular gloss of polypropylene abraded surfaces has been characterized by means of a three-angle glossmeter DRLANGE REFO 3-D in agreement with the ASTM D523, DIN 67530, and ISO 2813 specifications. The main principle of

this device is based on the idea of measuring the specular amount of reflected light directed to a surface at a specified angle from its normal. The three-angle glossmeter used in this investigation casts a white light beam at an angle of 20°, 60°, or 85° and a detector records the amount of reflected intensity in the specular direction (called also the mirror direction). The amount of light reflected from the surface under investigation is divided by the amount of light reflected from the surface of a reference smooth black glass plate (delivered by the manufacturer of the glossmeter) and the specular gloss is obtained by multiplying this intensity ratio by 100. Thirty measurements have been carried out onto the abraded surface of each polypropylene sample.

Statistical Treatment of the Experimental Results

Because of the numerous existing roughness parameters, it is not obvious to specify which of them is the most relevant for characterizing the topography of the overall polypropylene abraded surfaces under investigation in this study [8]. In this specific computer process, the relevance of each roughness parameter r_i is estimated by calculating the value of the Treatment Index F_i by means of the usual one-way analysis of variance (ANOVA) [12]. The Treatment Index F_i is used for comparing the factors of the total deviation. Its definition is given by

$$F_i = \frac{Variance\ of\ the\ i^{th}\ roughness\ parameter\ between\ samples}{Variance\ of\ the\ i^{th}\ roughness\ parameter\ of\ all\ samples} \quad (1)$$

More precisely, let us note $r_{i,s,n}$ the value of the roughness parameter r_i obtained from the n^{th} measurement ($n \in [1,N]$; N being the number of measurements performed on each surface equal to 50 in this investigation) on the s^{th} surfaces ($s \in [1,S]$; S being the number of studies equal to 7 in this investigation), $\bar{r}_{i,s}$ is the mean of the r_i roughness parameter of the s^{th} surface and $\bar{r}_i$ is the mean of i^{th} roughness parameter for all measurements performed on the overall surfaces. Then, the equation of variance analysis represents that the total sum of squares (SS_T) is the sum of the "between surface sum of squares" (SS_B) and the "within surface" sum of squares (SS_W) and is given by

$$\sum_S \sum_N \left(r_{i,s,n} - \bar{r}_i\right)^2 = N \sum_N \left(\bar{r}_{i,s} - \bar{r}_i\right)^2 + \sum_S \sum_N \left(r_{i,s,n} - \bar{r}_{i,s}\right)^2 \quad (2)$$

$$So\ F_i\ \ is\ \ given\ \ by\ F_i = \frac{\left(N \sum_N \left(\bar{r}_{i,s} - \bar{r}_i\right)^2\right)/(S-1)}{\left(\sum_S \sum_N \left(r_{i,s,n} - \bar{r}_{i,s}\right)^2\right)/(NS-S)} = \frac{MSB_i}{MSW_i} \quad (3)$$

If the i^{th} roughness parameter r_i does not discriminate the S surfaces, then MSB_i and MSW_i will be very similar (and $F_i \approx 1$). On the other hand, if the i^{th} roughness parameter r_i discriminates surfaces, then $MSB_i > MSW_i$ (and $F_i > 1$).

The related confidence interval of F_i is assessed by means of the Computer Based Bootstrap Method (CBBM). This new statistical treatment of experimental results we developed in our team several years ago was called "the Bootstraped Analysis of Variance."

As far as the CBBM is concerned, it should be remembered that, briefly speaking, this statistical method is based on the mathematical resampling technique and its main advantage is to allow the replacement of statistical inference assumptions about the underlying population by intensive calculations on a computer. In practice, the CBBM consists of generating a high number B of simulated bootstrap samples by perturbing the original scores of a given experimental data set of size N. A bootstrap sample of size N indexed by b, $b \in [1,B]$, and noted $(x_1^b, x_2^b, ..., x_N^b)$, is a collection of N values simply obtained by randomly sampling with replacement from the experimental data scores $(x_1, x_2, ..., x_N)$; each of them having a probability equal to $1/N$ to be selected. A bootstrap sample contains, therefore, scores of the experimental data set; some appearing zero times, some appearing one, some appearing twice, and so on. For more details on the CBBM, the reader should refer to Refs. [11, 13–15].

In this investigation, the CBBM was combined to the usual one-way ANOVA to identify with this first computer routine which roughness parameter is the most relevant to discriminate the different degree of abrasion of the polypropylene surfaces generated by the different paper grades. The CBBM was also combined to a correlation indicator of regression C_i related to the roughness parameter r_i to identify with a second computer routine which one is the most relevant to model the physical interaction of white light beam with a polypropylene abraded surface. Linear and exponential regressions were hypothesized to model this physical interaction.

IDENTIFICATION OF THE MOST RELEVANT ROUGHNESS PARAMETER DISCRIMINATING THE MORPHOLOGY OF POLYPROPYLENE ABRADED SURFACES

Conventional Analysis

This conventional analysis consists in studying a restrictive set of roughness parameters usually considered as relevant in literature either to characterize the surface topography of industrial products or to model the physical interactions of a surface with an optical wave. So, the first set of preselected roughness parameters includes the arithmetic average roughness R_a, the number of peaks per inch N_p, the root mean square roughness R_q, the mean slope of profiles Δa, the autocorrelation length L_{ac}, and also the fractal dimension Δ_{ANAM} estimated by a method developed by the authors [16, 17]. This method is called the average autocorrelation normalized method (ANAM) and is briefly summarized in **Appendix A**.

In this way, Fig. 2 shows the evolution of all these preselected roughness parameters with paper grade. Except for paper grade 80, it can be noted that when the number of abrasive grains per cm^2 increases, as expected, the values of the amplitude roughness parameters R_a and R_q decrease. Indeed, the higher the number of abrasive grains par cm^2, the lower the depth of the scratches. Besides, the number of peaks per inch N_p increases, the mean slope of profiles Δa decreases, the autocorrelation length L_{ac} decreases, whereas the fractal dimension Δ_{ANAM} increases. At this stage, the logical outcome of this conventional analysis would be to proceed to a one-way ANOVA analysis to determine which roughness parameter is the most relevant to characterize the overall polypropylene abraded

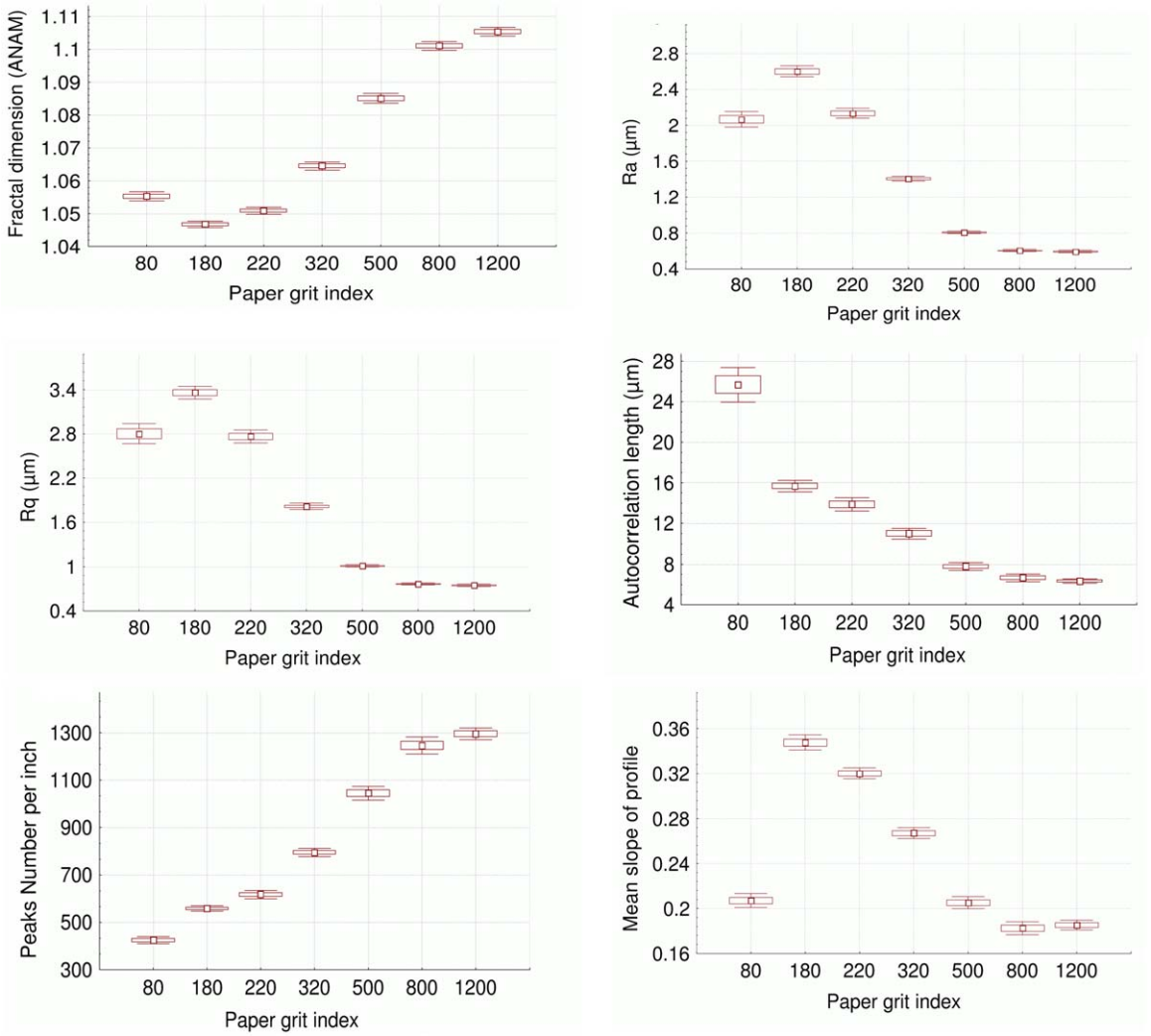

FIG. 2. Value of roughness parameters (fractal dimension, R_a, R_q, autocorrelation length, number of peaks, and mean slope of profile) versus the paper grit index. The square bracket represents the 95% confidence interval of the mean. [Color figure can be viewed in the online issue, which is available at wileyonlinelibrary.com.]

surfaces. For memory, the higher the calculated Treatment Index F_i, the most relevant the related roughness parameter r_i.

However, because of the numerous existing roughness parameters, there is no objective reason to claim that the most relevant one belongs to the short list of preselected parameters based on *a priori* knowledge. Besides, it must be added that the one-way ANOVA does not take into consideration the fact that a small perturbation in any score of the experimental data set can influence the value of the calculated Treatment Index F_i. In other words, for each roughness parameter, a confidence interval on the Treatment Index F_i should be assessed to build a robust statistical ranking of the overall values in order to affirm in a statistical sense which of these parameters is the most relevant.

Bootstraped ANOVA

The two limits aforementioned in the previous section can be overcome with the first computer routine we developed to carry out automatically an original statistical treatment combining the ANOVA with the CBBM (we called "Bootstraped ANOVA") taking into consideration more than a hundred of roughness parameters.

So, this computer routine was applied not only to the short list of preselected roughness parameters already presented but also to an extended list of a hundred of roughness parameters. (The algorithm is described in Figure C of Annex 3.) To build a confidence interval on the Treatment Index F_i related to a given roughness parameter r_i, the one-way ANOVA has been applied onto a high number of simulated Bootstrap sample B ($B = 10^6$ in this study) to obtain an empirical probability density function (PDF) consisting of a set of B simulated values of the Fisher Treatment Index noted $\left\{F_i^b;\, b \in [1, B]\right\}$. From this empirical PDF, it is finally possible to extract statistics like the mean of the Fisher Treatment Index $\overline{F_i}$ as well as the 5^{th} and 95^{th} percentiles, respectively, denoted as $F_i^{5\%}$ and $F_i^{95\%}$ to assess both the central tendency and the deviation through the calculation of the 90% confidence level.

This statistical procedure has been applied for the overall studied roughness parameters. It should be remembered that the higher the value of $\overline{F_i}$, the higher the relevance of the roughness

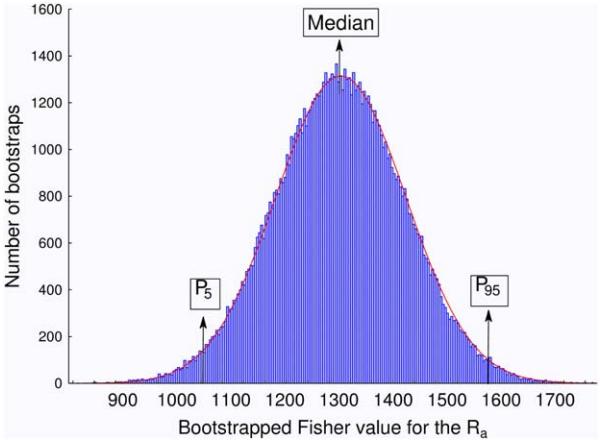

FIG. 3. Histograms of the F Fisher value obtained from 1,000,000 of bootstrap corresponding to the roughness parameter R_a. [Color figure can be viewed in the online issue, which is available at wileyonlinelibrary.com.]

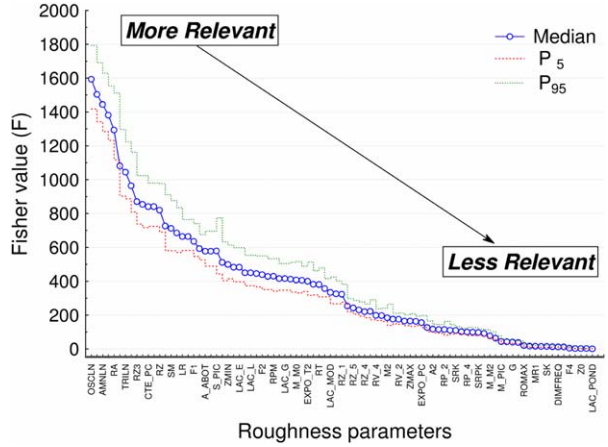

FIG. 4. Relevance graph for all roughness parameters ranked in a decreasing order relatively to the value of the Fisher Treatment Index F. [Color figure can be viewed in the online issue, which is available at wileyonlinelibrary.com.]

parameter r_i to discriminate the topography of the overall polypropylene abraded surfaces. Figure 3 illustrates the results obtained in the case of the amplitude roughness parameter R_a and Fig. 4 shows the final ranking considering the overall studied roughness parameters. In the final ranking, the roughness parameters L_{ac}, Δa, N_p, R_q, R_a, and Δ_{ANAM} rank, respectively, in 26th, 19th, 10th, 7th, 5th, and 2nd positions. Furthermore, it can be noted that among the hundred studied roughness parameters, the most relevant of them to discriminate the topography of the overall polypropylene abraded surfaces is the fractal dimension of the profiles. Indeed, OSCLN, BIGLN, AMNLN, and TRICCORI denote the four different methods to evaluate the fractal dimension of a profile. It should be remembered that the fractal dimension is a measure of the degree of tortuosity of a profile or a surface. The higher the fractal dimension, the more tortuous or chaotic is the profile or the surface.

IDENTIFICATION OF THE MOST RELEVANT ROUGHNESS PARAMETER MODELING THE PHYSICAL INTERACTION BETWEEN A WHITE LIGHT BEAM AND POLYPROPYLENE ABRADED SURFACES

Figure 5 shows the influence of the degree of abrasion damage due to the paper grade on the specular gloss measured at 60° and 85°. The objective here is to identify a relation between these values of specular gloss and the values of roughness parameters recorded independently onto the different polypropylene abraded surfaces. Even if the specular gloss are 2D measurements, it should be remembered that the roughness parameters were obtained from a large number of profiles measurements recorded randomly in various directions. In these conditions, as illustrated in Fig. 6 in the case of specular gloss values recorded at 60° and the roughness parameter R_a, only the mean values of these variables are simple to take into consideration when looking at a potential correlation; the major difficulty being to select a relevant model having a physical sense.

Two models have been considered with regard to the hundreds of roughness parameters assessed in this investigation: a simple linear regression and a more complicated exponential regression. The last one is a generalization to all the roughness parameters of the relation identified by Sandoz [18] between the specular gloss (G) and the roughness parameter R_q:

$$G = \alpha_i . e^{r_i} + c_i \tag{4}$$

where r_i is the i^{th} roughness parameter and (α_i, c_i) are constant

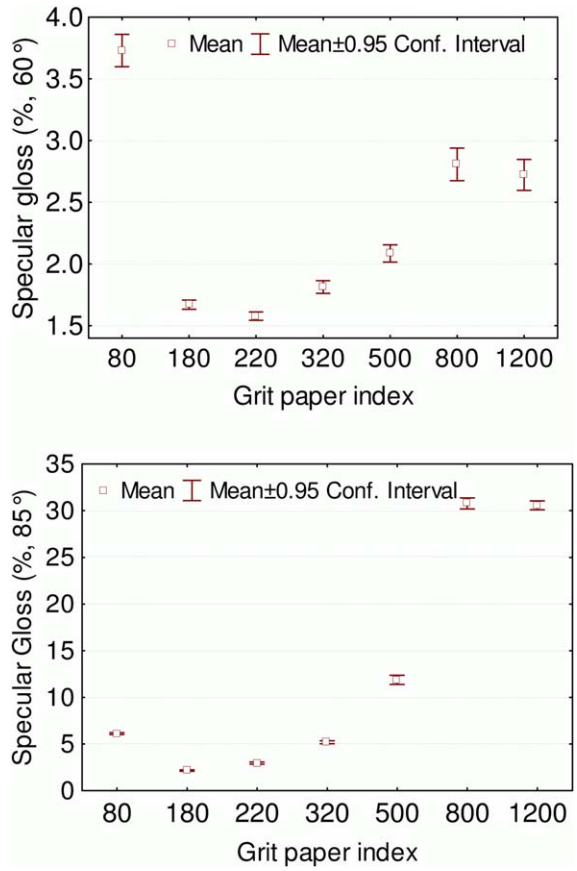

FIG. 5. Influence of the paper grit index on the specular gloss measured at 60° and 85°. [Color figure can be viewed in the online issue, which is available at wileyonlinelibrary.com.]

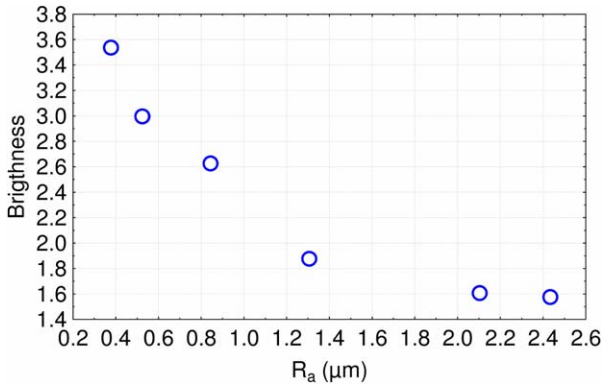

FIG. 6. Plot of the specular gloss values recorded at 60° versus the roughness parameter R_a values. [Color figure can be viewed in the online issue, which is available at wileyonlinelibrary.com.]

However, such an analysis remains usual and it is proposed in this investigation to combine again the CBBM to assess the relevance of the selected correlation model whether it is linear or not. The major interest of this original statistical analysis is to consider not only the means of the variables under consideration (i.e., the specular gloss and the selected roughness parameter) but also their variability.

Let us consider the case of the linear correlation to illustrate this original statistical analysis. Whatever the paper grade g ($g = 80$, 180, 220, 320, 550, 800, 1200) in which the measurements have been carried out, the experimental data set contains 60 values $(G_1, G_2, \ldots, G_{60})_g$ of specular gloss and 50 values $(r_{i,1}, r_{i,2}, \ldots, r_{i,50})_g$ of the i^{th} roughness parameter r_i under consideration (the algorithm is described in Figure D of Annex 3). The simulated Bootstrap samples obtained by randomly sampling with replacement scores of the experimental data set are, respectively, noted as $(G_1^b, G_2^b, ..., G_{60}^b)_g$ and $(r_{i,1}^b, r_{i,2}^b, ..., r_{i,50}^b)_g$; the superscript b refers to the b^{th} Bootstrap simulation. The means of these newly simulated samples are then calculated for each paper grade g and are respectively noted as $\overline{(G^b)_g}$ and $\overline{(r_i^b)_g}$. These means are reported on a graph $\overline{(G^b)_g} = f\left(\overline{(r_i^b)_g}\right)$ from which a slope noted α_i^b can be determined if a linear correlation is assumed between the variables. Repeating this procedure B times ($B = 1{,}000$ in this investigation) leads to a set of B slope values $\left\{\alpha_i^b;\, b \in [1, B]\right\}$ that can be plotted to obtain an empirical probability density function (PDF) related to the i^{th} roughness parameter r_i under consideration. Figure 7 shows the examples of PDF obtained for the different preselected roughness parameters considering specular gloss measurements at 60° and 85°.

Whatever the PDF, it is possible to extract the mean $\overline{\alpha_i}$ as well as the 5$^{\text{th}}$ and 95$^{\text{th}}$ percentiles $\alpha_i^{5\%}$ and $\alpha_i^{95\%}$ to assess a 90% confidence interval equal to $\alpha_i^{95\%} - \alpha_i^{5\%}$. These statistical estimations are used to define an unscaled coefficient C_i^b related to the roughness parameter r_i and the b^{th} Bootstrap simulation:

$$C_i^b = \frac{\alpha_i^b}{\alpha_i^{95\%} - \alpha_i^{5\%}} \tag{5}$$

Let us note $\overline{C_i}$ the mean value of C_i^b defined by

$$\overline{C_i} = \frac{\overline{\alpha_i}}{\alpha_i^{95\%} - \alpha_i^{5\%}} \tag{6}$$

We called this variable $\overline{C_i}$ the correlation power related to the i^{th} roughness parameter r_i. The higher the value of $\overline{C_i}$, the more relevant the i^{th} roughness parameter r_i to model the physical interaction of a white light beam with a polypropylene abraded surface.

Figure 8a shows the final ranking of the power correlation in a decreasing order for the overall studied roughness parameters when assuming a linear correlation between the specular gloss and the roughness parameters. Figure 8b shows the evolution of the ranking obtained when assuming an exponential regression as presented in equation *4*. It should be mentioned that Fig. 8a and b refers to specular gloss measurements at 85° that lead to higher power correlation values. Looking at these figures, it can be concluded that the fractal dimension remains again the most relevant roughness parameter to model the physical interaction of a white light beam with a polypropylene abraded surface. Moreover, the power correlation values obtained are higher considering the exponential regression in comparison to the linear one. In other terms, in agreement with the results of Sandoz, the exponential r regression is more relevant than the linear one to

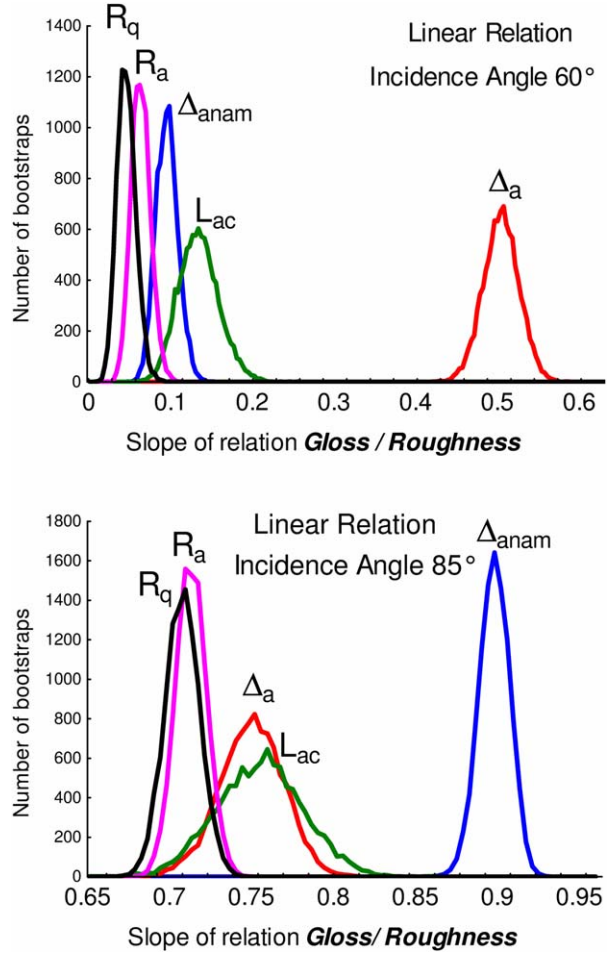

FIG. 7. Examples of PDF obtained for the different preselected roughness parameters considering specular gloss measurements at 60° and 85°. [Color figure can be viewed in the online issue, which is available at wileyonlinelibrary.com.]

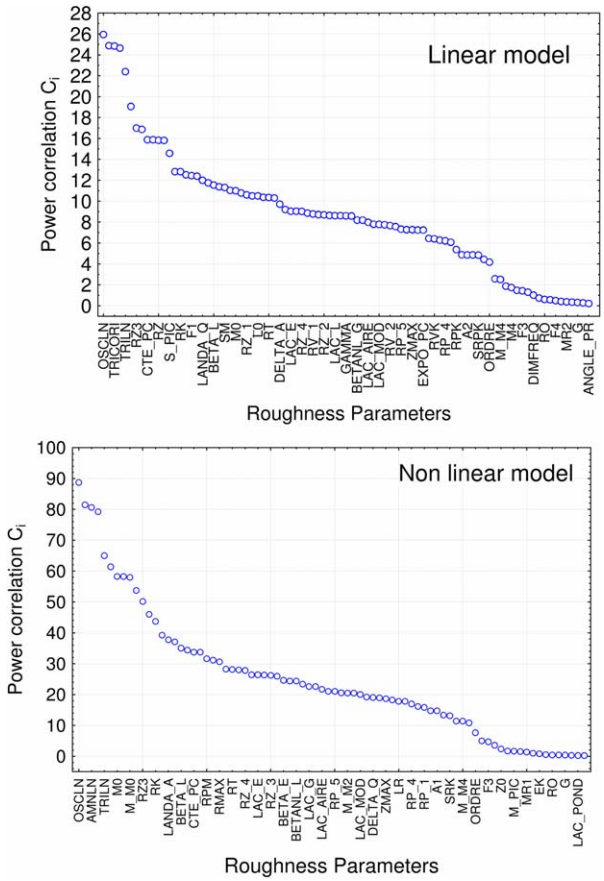

FIG. 8. Final ranking of the power correlation (using linear or exponential models) in a decreasing order for the overall roughness parameters considered in this investigation. [Color figure can be viewed in the online issue, which is available at wileyonlinelibrary.com.]

model the physical interaction of a white light beam with a polypropylene abraded surface. Such model is presented on Fig. 9 revealing that the specular gloss increases with the fractal dimension of the polypropylene abraded surface.

INTERPRETATION OF THE EXPERIMENTAL RESULTS

The roughness of machined surfaces is of prime importance across a very wide spectrum of industrial applications. Indeed, the morphology of machined surfaces often influences the properties that govern the application of the manufactured product. Because of these various industrial but also scientific interests, a proliferation of roughness parameters, possibly running into hundreds, has been triggered to describe the different kinds of surface morphology with regard to specific functions, properties, or applications. In spite of this proliferation, termed by Whitehouse the "parameter rash," there is still no complete comprehensive account for the relevance of these roughness parameters [8, 10]. A major problem is therefore in many cases to determine quantitatively, and without preconception, the most relevant roughness parameter that characterizes the surface morphology of a manufactured product with regard to a correlation with a particular function, property, or application.

Using our computer routine MESRUG that we specifically developed several years ago to address this problem, it is shown in the present investigation that, among a hundred of roughness parameters, the fractal dimension is the most relevant to discriminate the surface morphologies of different abraded polypropylene abraded surfaces and to describe the physical interactions between these surfaces and a white light beam. Our experimental results show that the higher the paper grade, and consequently, the number of abrasive grains per cm^2, the lower the values of the amplitude roughness parameters R_a and R_q as well as the mean slope of the profiles Δa. Such expected results are in agreement with the fact that the higher the number of abrasive grains per cm^2, the lower the depth of the scratches generated randomly at the polypropylene surface by using an automatic grinding machine. Besides, the results also show that an increase of the number of peaks per inch N_p increases with the paper grade. This means that the noise related to the amplitude of the profiles increases when the number of abrasive grains per cm^2 increases. In these conditions, hence it is no surprise that the higher the paper grade, the more pronounced is the tortuous or chaotic aspect and the higher the fractal dimension of the abraded polypropylene surface estimated by the ANAM.

Furthermore, numerous existing models describing the physical interaction of optical waves and the surface morphology are derived from Beckmann's and Spizzichino's pioneering work [19]. By far, the largest numbers of these models are based on the Kirchhoff approximation of the boundary conditions, which are required to evaluate the Helmholtz integral. Considering these approximations for perfectly conducting rough surfaces generated by random processes (such surfaces can be described by their Gaussian statistical distributions and correlation function), Beckmann derived the following formula from the calculation of the Helmholtz integral [19]:

$$I/I_0 = \exp\left(-\left(\frac{4\pi R_q \cos\theta}{\lambda}\right)^2\right) + \frac{\lambda^2 {L_{ac}}^2}{16\pi A {R_q}^2 \cos^2\theta} \qquad (7)$$

where I/I_0 represents the ratio of the scattered intensity in the direction of specular reflection by the intensity of the incident

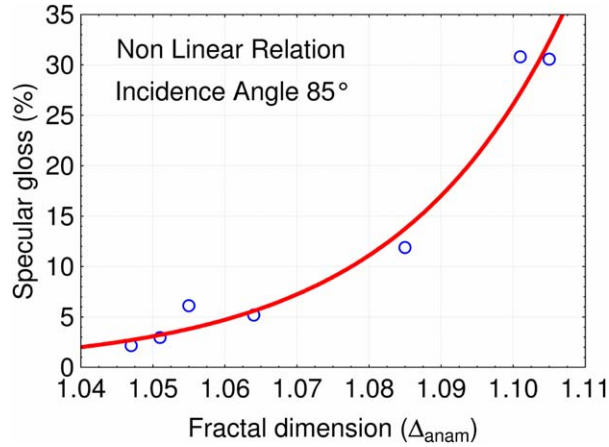

FIG. 9. Specular gloss versus fractal dimension of the polypropylene abraded surface considering the exponential model which is the most relevant (red curve). [Color figure can be viewed in the online issue, which is available at wileyonlinelibrary.com.]

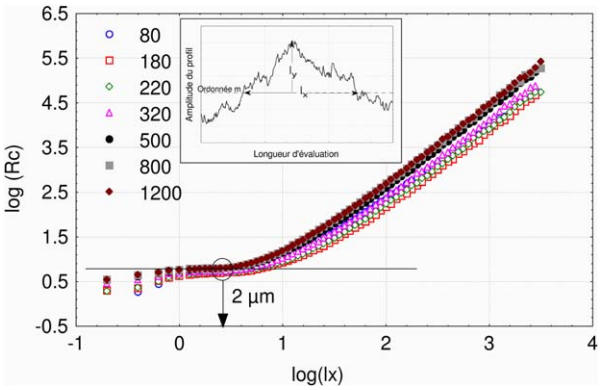

FIG. 10. Evolution of the fractal curvature radius R_c versus the scale l_x for all polished surfaces with different paper indexes (80, 180, 220, 320, 500, 800, and 1,200). [Color figure can be viewed in the online issue, which is available at wileyonlinelibrary.com.]

radiation, λ is the wavelength, θ is the incident angle, A is the scattering zone area, R_q is the root-mean squared roughness, and L_{ac} is the correlation length of the surface. The two terms of this relation correspond respectively to the specular and the diffuse components of the scattered light; the former dominates for smooth surfaces while the latter for rough surfaces.

In fact, most of the models derived from Beckmann's express the scattered intensity of an optical wave as a function of the scattering angle, the electromagnetic properties of the studied material, the wavelength, and commonly used surface parameters such as R_q and L_{ac}. In such models, numerous authors apply the Kirchhoff approximations in which the geometry of a surface asperity is described by its curvature radius r_{ci} that is assumed to be higher than the wavelength λ [19–23]. It must be pointed out that these models have been developed for periodically (sinusoidal or saw-tooth profiles) and random surface roughness.

Besides, wave interactions with fractal rough surfaces have also been studied more recently [20, 24–28]. However, as claimed by some authors, the notion of tangent plane necessary to estimate the Helmholtz integral and model the scattered intensity within Kirchhoff approximations does not exist anymore for a fractal representation of surface roughness which is intrinsically not differentiable. Our experimental results show without any ambiguity that the most relevant roughness to characterize the topography of a polypropylene abraded surface and to model its interaction with a white light beam is the fractal dimension. In these conditions, optical models based on the Kirchhoff approximations are not applicable to our experimental results.

To explain our experimental results showing that the specular gloss increases with the fractal dimension of the abraded polypropylene surface, it should be remembered that a chaotic profile has a high dimension; a white noise profile having a maximal fractal dimension equal to 2. A surface with a low noise relatively to its roughness amplitude will have a low fractal dimension, a strong propensity to diffuse the scattered light and, as a consequence, a low specular gloss. On the contrary, a surface with a high noise relatively to its roughness amplitude will have higher fractal dimension and specular gloss.

In the last part of this discussion, we proposed an attempt is presented to link optical models developed for perfectly rough surfaces perfectly conducting rough surfaces generated by random processes and based on Kirchoff approximation and those proposed for fractal surfaces. This attempt consists in extending the classical definition of the asperities radii calculation presented in the Nowicki's work to a generalized one introducing a fractal concept of curvature radii of surfaces that depends on the observation scale. Hence we have recently proposed a new method of roughness peaks curvature radii calculation (see Annex 2) and applied it successfully to some tribological applications [29]. It should be mentioned that this fractal concept of curvature radii of surfaces also numerically depends on horizontal lines intercepted by the studied profile. It is then established the increasing of the measures dispersion due to that lines with that of the corresponding radii and the dependence on calculated radii on the fractal dimension of the studied curve. Consequently, the notion of peak and its associated curvature are mathematically reformulated. For fractal curves, the curvature radius r_c depends on the scale at which the observation is made.

Figure 10 presents the evolution of the radii curvature r_c versus the length of observation l_x for the overall abraded polypropylene surfaces under investigation. As it can be observed, radius r_c follows a power law related to the fractal dimension of the surfaces varying for the different paper grades. The higher the scale of observation l_x, the higher the radii curvature r_c. To select the appropriate scale of observation l_x, a value near the wavelength of the white light is chosen. As a consequence, we will retain to analyze more precisely the value of the fractal radii curvature at the scale of 1 µm. Figure 11 presents the gloss versus the fractal radius curvature r_c for $l_x = 1$ µm. As it can be observed, a linear positive relation emerges in log–log plot meaning that the higher the fractal radii curvature, the higher the gloss. An important fact has to be pointed out: the surfaces polished with high paper grades show peaks with high fractal radius curvature. At the contrary, surfaces polished with low paper grades show peaks with low radius curvature. Moreover, our experimental results revealed that the surfaces polished with paper grade 80 were less rough than those polished with paper

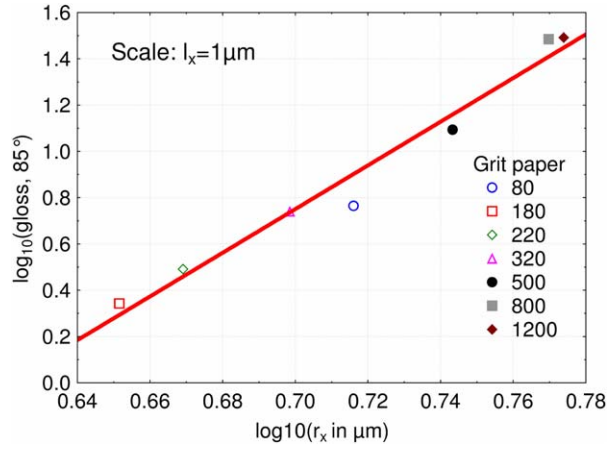

FIG. 11. The brightness versus the fractal radius curvature estimated at the scale of 1 µm for all polished surfaces with different paper indexes (80, 180, 220, 320, 500, 800, and 1,200). [Color figure can be viewed in the online issue, which is available at wileyonlinelibrary.com.]

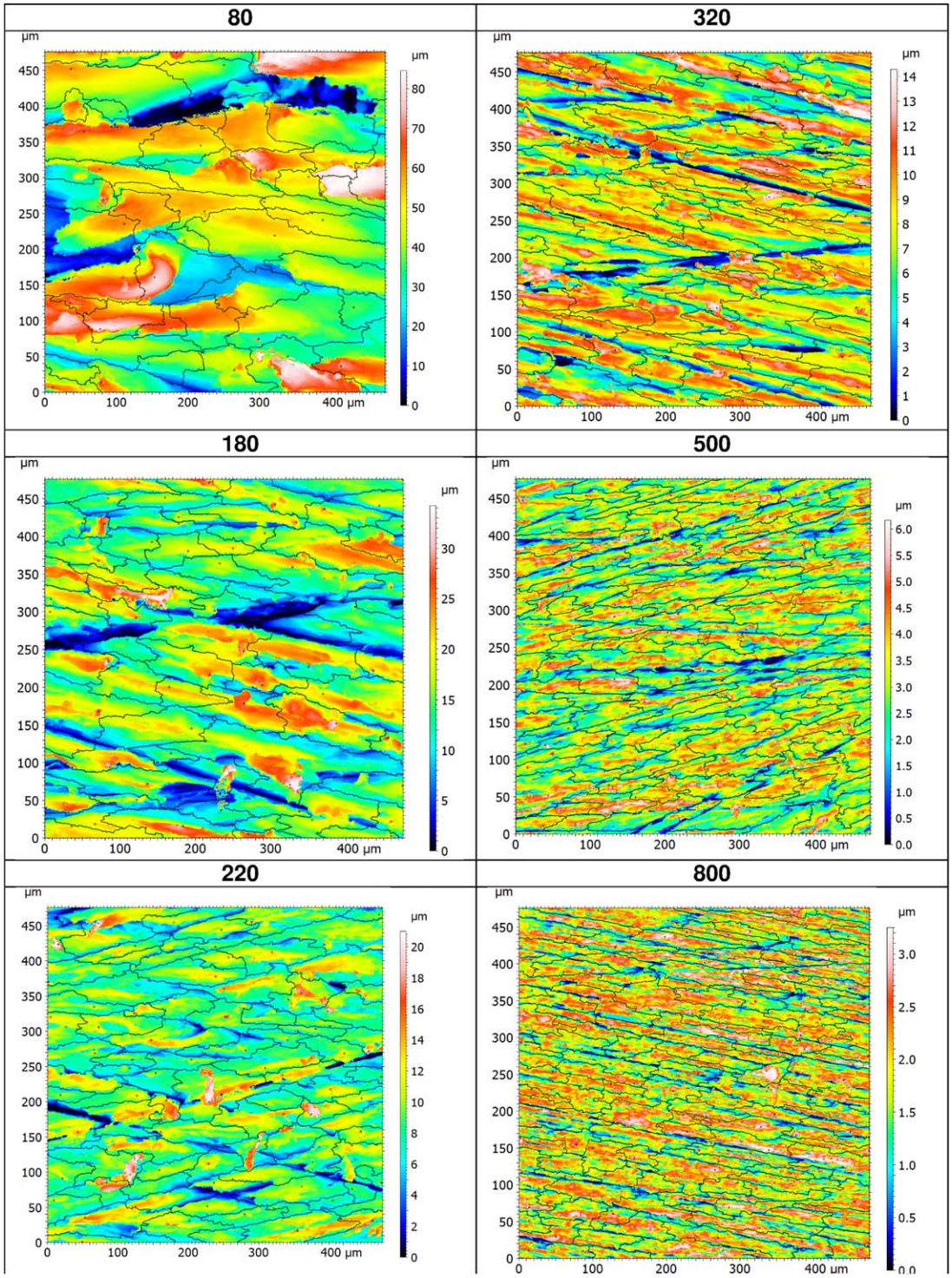

FIG. 12. 3D Roughness map for polypropylene surfaces abraded with grit size paper 80, 180, 220, 320, 500, and 800 including motifs decomposition. [Color figure can be viewed in the online issue, which is available at wileyonlinelibrary.com.]

220. As it can be observed in Fig. 11, this surface has a higher gloss and follows the linear log–log relation. This clearly means that the gloss of an abraded polypropylene surface is closely related to the fractal aspect of its topography. When peak sizes are small relatively to the light wavelength, the classical Kirchhoff hypothesis fails. However, taking into account the fractal aspect of radii curvature, the following result emerges: the higher the fractal radii curvature of the peaks of the surface, the higher its gloss.

Furthermore, we have proved that $r_c(l_x) \propto l_x^{\Delta}$ [30]. If l_x is fixed at the scale of the wavelength, increasing the fractal dimension will then increases the fractal radii curvature of the peaks. This point explains our result showing that the gloss of an abraded polypropylene surface increases with the fractal

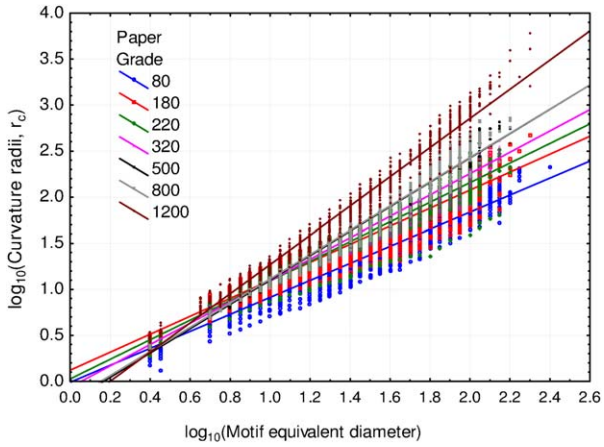

FIG. 13. Evolution of the 3D fractal curvature radius of motif r_c versus the equivalent diameter of motifs for all polished surfaces with different paper indexes (80, 180, 220, 320, 500, 800, and 1,200). [Color figure can be viewed in the online issue, which is available at wileyonlinelibrary.com.]

dimension of its topography. The main criticism of our approach is that applying 2D roughness from profiles whereas the surface should be characterized by a 3D roughness could be appearing as meaningless. However, it should be remembered firstly that the 2D profiles have been recorded randomly onto the surfaces of the different studied samples. Second, a 3D approach can be proposed. The main problem consists in defining a radii curvature of a peak on a 3D topographical map. So we have proceeded to 3D measurements on new polished samples (different polypropylene microstructures that those used in the 2D analyses).

Figure 12 presents the 3D topographical maps. Then the Wolf Pruning algorithm [31] is applied with different thresholds to obtain motifs decomposition. From each motif, the height (h) and the equivalent diameter (ϕ) is computed. We have proved that the 3D radii curvature $r_c(\phi)$ is given by $r_c(\phi)=\phi^2/8h$ and leads to the power law $r_c(\phi) \propto \phi^{\Delta}$ where Δ is the fractal dimension (results to be published). Figure 13 presents the fractal evolution of the 3D radii curvature versus the motif equivalent diameter. The slope in the log–log coordinate gives the fractal dimension. Similar to that in 2D measurements, when

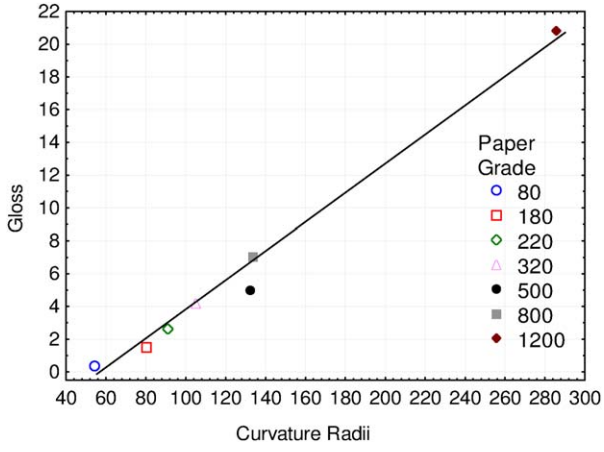

FIG. 14. The brightness versus the 3D fractal radius curvature for all polished surfaces with different paper indexes (80, 180, 220, 320, 500, 800, and 1,200). [Color figure can be viewed in the online issue, which is available at wileyonlinelibrary.com.]

fractal dimension of surfaces increases, gloss increases. This increase is also related to an increase of the fractal radii curvature of the surface (Fig. 14).

CONCLUSIONS

Thanks to an original methodology combining the Computer Based Bootstrap Method to conventional statistical analyses we developed, it was found that, among a hundred of roughness parameters, fractal dimension is the most relevant one to discriminate the topographies of polypropylene abraded surfaces and to model the physical interaction of a white light beam with these surfaces. It was shown that an exponential correlation between gloss and fractal dimension of a polypropylene abraded surface was more relevant than a linear one.

Besides, we proposed an attempt to link optical models developed for perfectly rough surfaces perfectly conducting rough surfaces generated by random processes and based on Kirchoff approximation and those proposed for fractal surfaces. This attempt consists in extending the classical definition of the asperities radii calculation presented in the Nowicki's work to a generalized one introducing a fractal concept of curvature radii of surfaces that depends on the observation scale. It is shown that the fractal dimension of an abraded surface is correlated to the local curvature radii of its peaks estimated at the scale corresponding to wavelength of the white light beam.

The higher the fractal dimension of a surface, the higher the fractal radii curvature of its peaks. This point explains our results showing that the gloss of a polypropylene surface increases with its fractal dimension.

As fractal dimension described well the gloss measurements, a multiscale analysis will be performed in the future to well describe the different scale effects.

APPENDIX A: ESTIMATION OF THE FRACTAL DIMENSION OF A PROFILE BY THE AVERAGE AUTOCORRELATION NORMALIZED METHOD (ANAM)

Let us consider $a < b$ where a and b are two real numbers, f and C^0 function such that $f : [a-\tau, b+\tau] \rightarrow IR$, $x \rightarrow f(x)$. Let us generalize the structure function with α a real number higher than unity and define $M_\tau^\alpha(f,x)$ as follows:

$$M_\tau^\alpha(f,x)=\left[\frac{1}{\tau^2}\int_{t_1=0}^{\tau}\int_{t_2=0}^{\tau}|f(x+t_1)-f(x-t_2)|^{\alpha}\,dt_1\,dt_2\right]^{\frac{1}{\alpha}}$$

By averaging $M_\tau^\alpha(f,x)$ on the overall profile length L, the $K_\tau^\alpha(f,L)$ function is formally obtained:

$$K_\tau^\alpha(f,L)=\frac{1}{L}\int_{x=0}^{x=L}\left[\frac{1}{\tau^2}\int_{t_1=0}^{\tau}\int_{t_2=0}^{\tau}|f(x+t_1)-f(x-t_2)|^{\alpha}\,dt_1\,dt_2\right]^{\frac{1}{\alpha}}dx$$

The numerical form of this equation is given below:

$$\hat{K}_{k\,\delta x}^{\alpha}(f,n)=\frac{(k+1)^{-\frac{2}{\alpha}}}{n-2k}\sum_{i=k+1}^{n-k}\left[\sum_{j=0}^{k}\sum_{l=0}^{k}|f_{i+j}-f_{i-l}|^{\alpha}\right]^{\frac{1}{\alpha}}$$

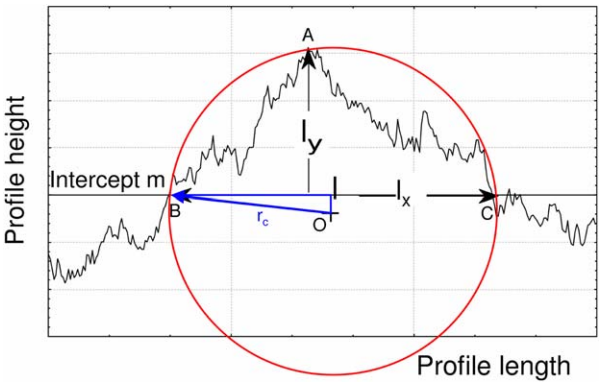

FIG. A. Definition of l_x and l_y used to calculate the local curvature radius $r_c(l_x)$. [Color figure can be viewed in the online issue, which is available at wileyonlinelibrary.com.]

where $n = L\delta x$ is the number of discretized consecutive points equally spaced of a distance $\delta x = x_{i+1} - x_i$ on the overall profile length L.

If the considered function f is assumed to be Hölderian and anti-Hölderian, it can be shown that

$$\Delta(f,L) = \lim_{\tau \to 0} \left(2 - \frac{\log K_\tau^\alpha(f,L)}{\log \tau}\right)$$

Finally, the fractal dimension is assessed using the linear least square method to calculate the slope of the plot $\log \hat{K}^{\alpha}_{k\,\delta x}(f,n)$ versus $\log(k\,\delta x)$ for various $k\delta x$ values; this slope corresponds to the Hölder exponent $H(f,L)$ and $\Delta(f,L) = 2 - H(f,L)$. The higher the fractal dimension, the higher the chaotic aspect of the profile.

APPENDIX B: EVALUATION OF THE RADIUS CURVATURE OF AN ASPERITY AS A FUNCTION OF THE OBSERVATION SCALE

To consider the potential fractal aspect of a profile, a new method is proposed to calculate the radius curvature r_{ci} of an asperity as a function of the observation scale. The different steps of this new method are listed below:

- (a) A horizontal line is fixed at a level h crossing the profile to obtain a set of l_{xi} values as defined below on Fig. A.
- (b) For each l_{xi} value, the related l_{yi} value that characterizes the local maximum height is computed.
- (c) Then, for each "peak," the calculation of r_{ci} is computed using the formula established by Nowicki [32]. These operations are repeated for each element of the set of l_{xi} values.
- (d) Another horizontal height is chosen and steps a to c are repeated. On the whole, one hundred equally spaced intercept lines covering the whole amplitude height range of the profile have been studied.

If the considered function f defined on $[a,b]$ is a nonconstant continuous functions uniformly Hölderian and anti-Hölderian [30], if l_x exists, then the fractal dimension of the profile is given by

$$\Delta(G_f) = \limsup_{l_x \to 0} \left(\log r_c(l_x)/\log l_x\right)$$

APPENDIX C: ALGORITHM OF THE BOOSTRAPED ANOVA

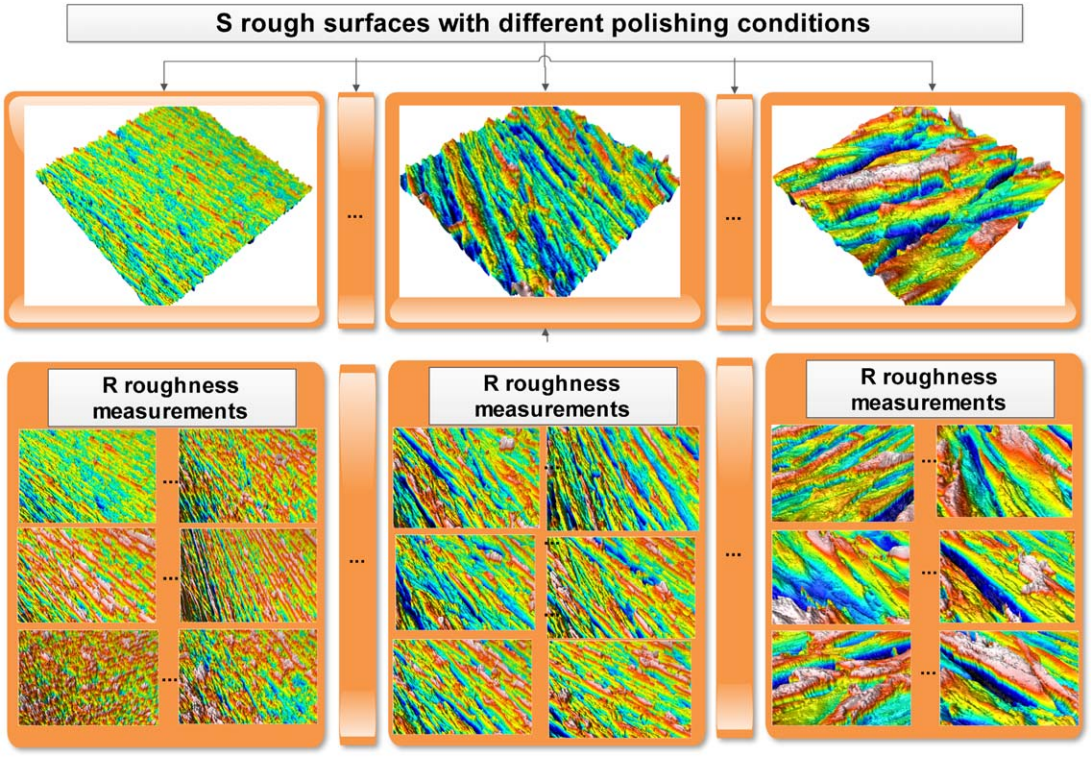

FIG. C. Synoptic of analyses of variance by a bootstrap method (1: sampling surfaces with replacement; 2: algorithm of relevance computation). [Color figure can be viewed in the online issue, which is available at wileyonlinelibrary.com.]

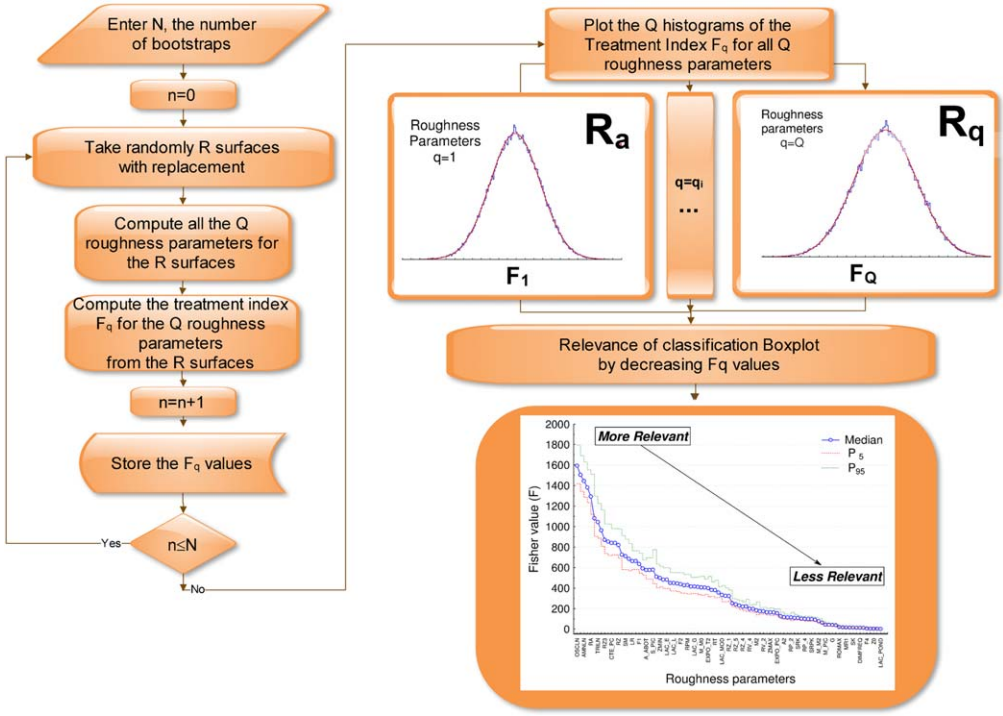

FIG. C. *Continued.*

APPENDIX D: ALGORITHM OF IDENTIFICATION OF THE MOST RELEVANT ROUGHNESS PARAMETER MODELING THE PHYSICAL INTERACTION BETWEEN A WHITE LIGHT BEAM AND POLYPROPYLENE ABRADED SURFACES

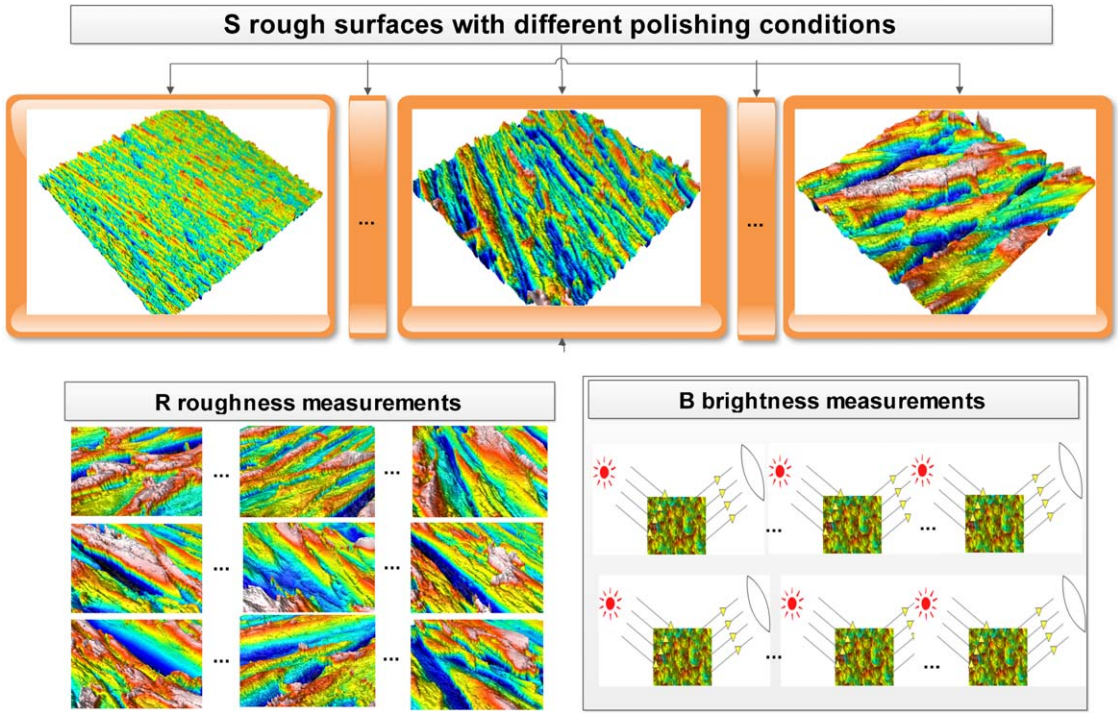

FIG. D. Synoptic of identification of the most relevant roughness parameter to model interaction between a white light beam and the surface topography by a bootstrap method (1: sampling surfaces and gloss measurement with replacement; 2: algorithm of bivariate bootstrapped distribution; 3: algorithm of relevance computation). [Color figure can be viewed in the online issue, which is available at wileyonlinelibrary.com.]

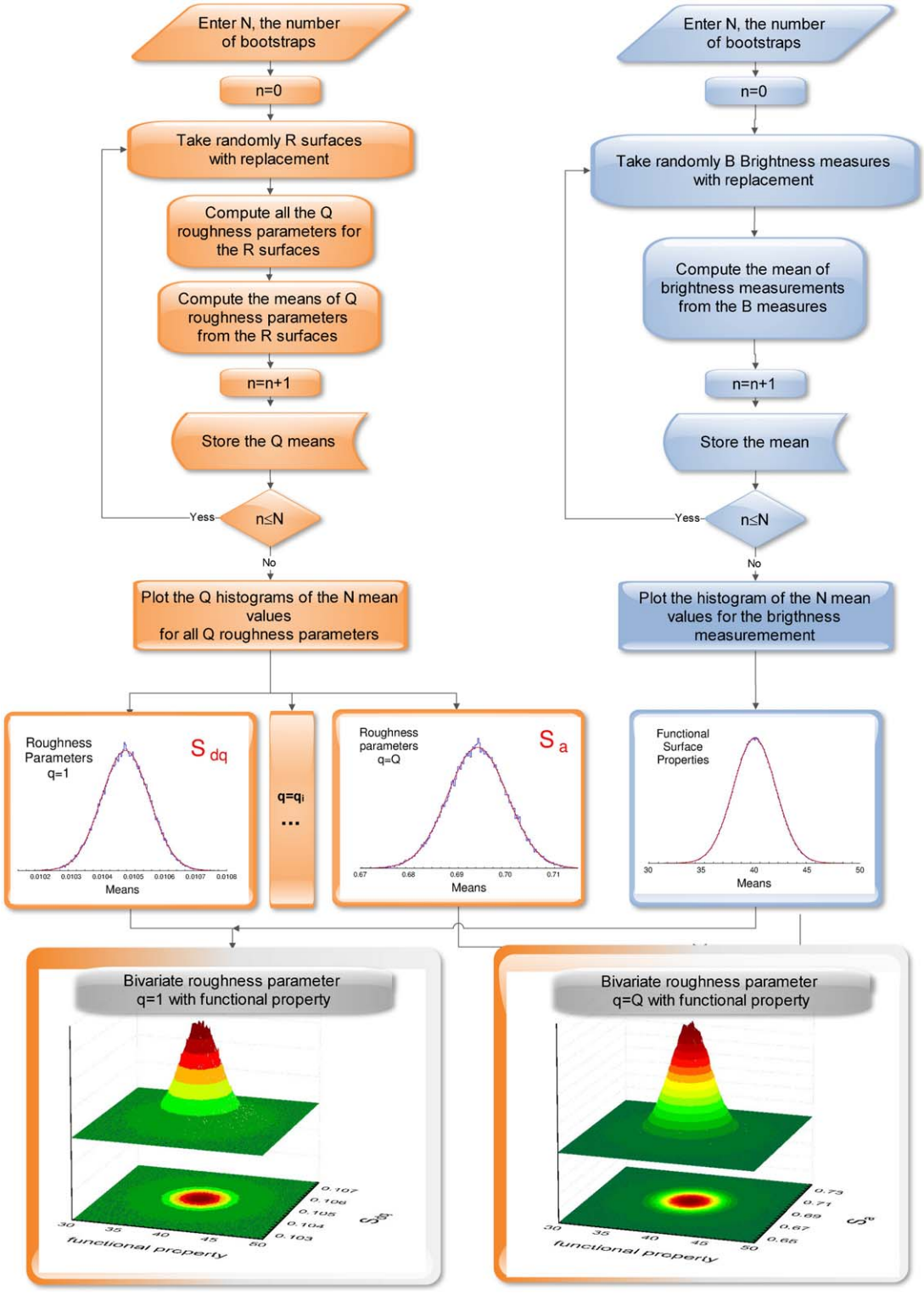

FIG. D. *Continued.*

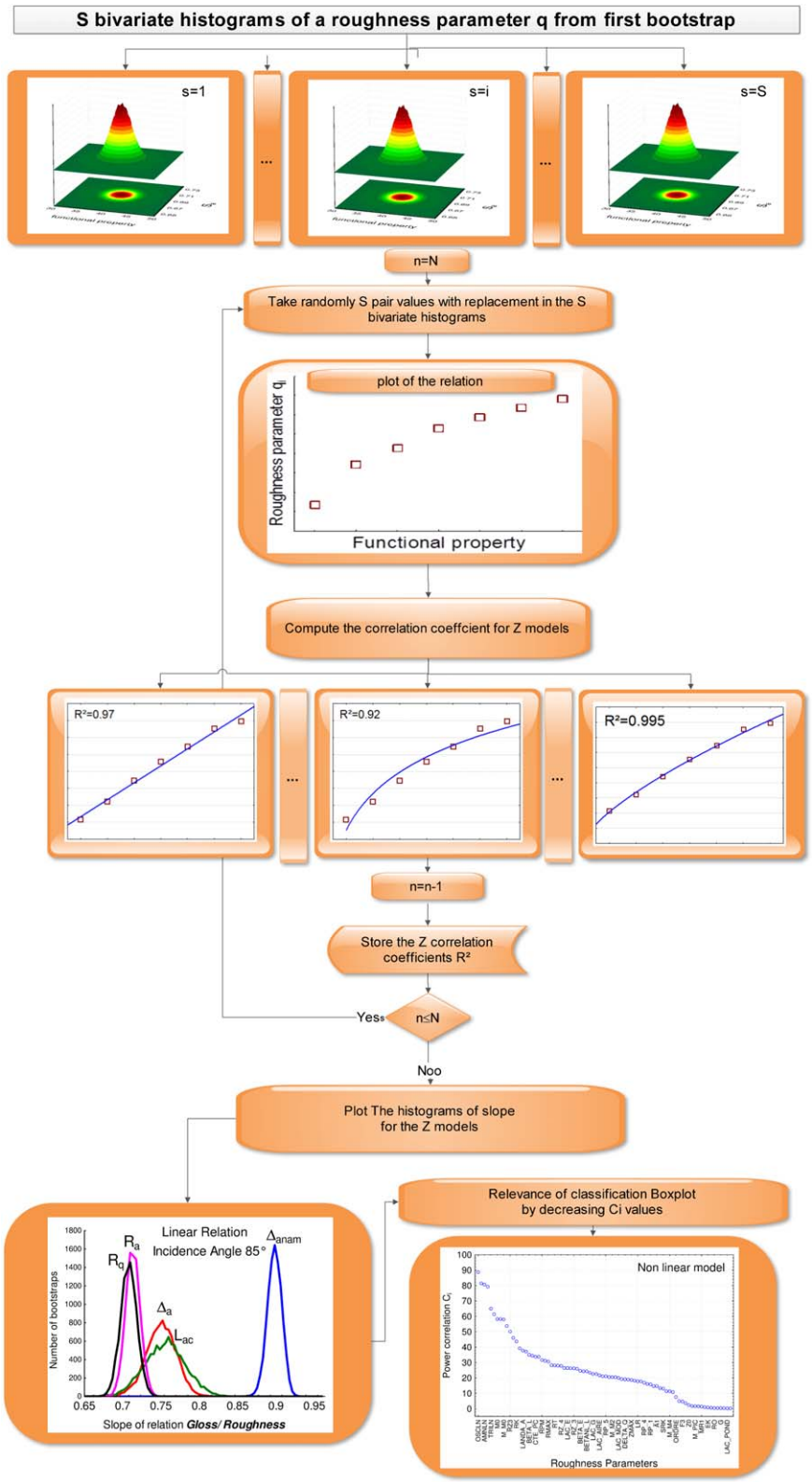

FIG. D. *Continued.*

REFERENCES

1. W.H. Mörmann, B. Stawarczyk, A. Ender, B. Sener, T. Attin, and A. Mehl, *J. Mech. Behav. Biomed. Mater.*, **20**, 113 (2013).
2. J. Da Costa, A. Adams-belusko, K. Riley, and J.L. Ferrecane, *J. Dentistry*, **385**, 123 (2010).
3. J. Eck, A.L. Kass, J.L.J. Mulders, and R. Goebel, *Acta Psycholog.*, **143**, 20 (2013).
4. W.M. Bergmann Tiest and A.M.L. Kappers, *Acta Psycholog.*, **124**, 177 (2007).
5. J. Järnström, P. Ihalainen, K. Backfolk, and J. Peltonen, *Appl. Surf. Sci.*, **254**, 5741 (2008).
6. V. Briones, J.M. Aguilera, and C. Brown, *J. Food Eng.*, **77**, 776 (2006).
7. J. Ferracane, S. Khajotia, K. Smart, and L. Ferracane, *Dental Mater.*, **25**, 19 (2009).
8. D.J. Whitehouse, *Wear*, **83**, 75 (1982).
9. M. Bigerelle, D. Najjar, and A. Iost, *Rev. Métall.*, 467 (2002).
10. M. Bigerelle, D. Najjar, and A. Iost, *J. Mater. Sci.*, **38**, 2525 (2003).
11. D. Najjar, M. Bigerelle, and A. Iost, *Wear*, **254**, 450 (2003).
12. G. Keppel and W.H. Sauffley, *Introduction to Design and Analysis*, W. H. Freeman and Company, New York, 1980.
13. B. Efron, *Ann. Stat.*, **7**, 1 (1979).
14. B. Efron and R.J. Tibshirani, *An Introduction to the Bootstrap*, Chapman and Hall, 1993.
15. P. Hall, *The Bootstrap and the Edgeworth Expansion*, Springer-Verlag, 1992.
16. M. Bigerelle and A. Iost, *C. R. Acad. Sci. Ser. II*, **323**, 669 (1996).
17. M. Bigerelle and A. Iost, *Comput. Math. Appl.*, **42**, 241 (2001).
18. P. Sandoz, G. Tribillon, T. Gharbi, and R. Devillers, *Wear*, **201**, 186 (1996).
19. P. Beckmann and A. Spizzichino, *The Scattering of Electromagnetic Waves from Rough Surfaces*, Pergamon Press, London, 1963.
20. P. Callet, *Couleur-Lumière Couleur-Matière: Interaction Lumière-Matière et Synthèse d'Images*, Diderot Editeur, Arts et Sciences, Paris, 1998.
21. J.C. Dainty, N.C. Bruce, and A.J. Sant, *Measurement of Light Scattering by a Characterized Random Rough Surface, Waves in Random Media*, in "An Institute of Physics Journal," Dainty J.C. and D. Maystre, Eds. **1**, 29 (1991).
22. A. Ishimaru, S.C. Jei, P. Phu, and K. Yoshitomi Numerical, Analytical and Experimental Studies of Scattering from Very Rough Surfaces and Backscattering Enhancement. Waves in Random Media, J.C. Dainty and D. Maystre editors, An Institute of Physics Journal, 1991; **1**:91–107.
23. D.L. Jaggard and X. Sun, *J. Opt. Soc.*, **A7**, 1131 (1990).
24. D.L. Jaggard Fractal electrodynamics: from super antennas to superlattices. in Fractals in Engineering, J.L. Vehel, E. Lutton and C. Tricot editors, Springer-Verlag, Berlin, 1997;204–221.
25. C.J.R. Sheppard, *Opt. Comm.*, **122**, 178 (1996).
26. E. Jakeman. Non-gaussian statistical models for scattering calculations. in Waves in Random Media, J.C. Dainty and D. Maystre editors, An Institute of Physics Journal, 1991;**1**:109–119.
27. E. Jakeman, *J. Phys.*, **A15**, L55 (1982).
28. R. Botet, E.Y. Poliakov, V.M. Shalaev, and V.A. Markel Fractal-surface-enhanced optical responses. in Fractals in Engineering, J.L. Vehel, E. Lutton and C. Tricot editors, Springer Verlag, Berlin, 1997; 237–251.
29. M. Bigerelle, J.M. Nianga, D. Najjar, A. Iost, C. Hubert, and K.J. Kubiak, *Trib. Int.*, **65**, 235 (2013).
30. M. Bigerelle. Caractérisation géométrique des surfaces et interfaces - Applications en métallurgie, PhD ENSAM, Lille 1999.
31. ISO 25178-2:2012. Geometrical product specifications (GPS) - Surface texture: Areal-Part 2: Terms, definitions and surface texture parameters.
32. B. Nowiki, *Wear*, **102**, 161 (1985).